and convergence rates from Table 1. We show the minimum slab temperatures at the depth of the increase of deep seismicity in each subduction zone in Figure 3. With the possible exception of Izu-Bonin, all deep seismicity increases occur beyond the $\alpha \to \alpha + \gamma$ transition within the slab, again consistent with the hypothesis that olivine phase transformations mediate deep seismicity. The overall pattern is one of two equally sized groups, one at the lower left lying close to the $\alpha \to \alpha + \gamma$ phase boundary and the other farther away. The former group's proximity to the phase boundary suggests that in some cases seismicity increases closely follow phase transformations. Whether these are due to the changes in the slab stress state caused by the phase transformation or due to an unchanged stress state in a new, weaker slab rheology is unclear. Whatever the mechanism, the idea that olivine phase transformations somehow control deep earthquakes is supported by the seismicity patterns in individual subduction zones. It is not, however, obvious how this occurs. □

1. Green, H. W., Young, T. E., Walker, D., Scholz, C. & Prior, D. Trans. Am. Geophys. Un. 71, 946 (1990).
2. Kirby, S. H. J. geophys. Res. 92, 13789-13800 (1987).
3. Green, H. W. & Burnley, P. C. Nature 341, 733-737 (1989).
4. Kirby, S. H., Durham, W. B. & Stern, L. A. Science 252, 216-225 (1991).
5. Kirby, S. H. Trans. Am. Geophys. Un. 71, 946 (1990).
6. Rubie, D. C. Nature 308, 505-508 (1984).
7. Lomnitz-Adler, J. J. Phys. Earth 38, 83-98 (1990).
8. Frohlich, C. Ann. Rev. Earth planet. Sci. 17, 227-254 (1989).
9. Akaogi, M., Ito, E. & Navrotsky, A. J. geophys. Res. 94, 15671-15685 (1989).
10. Brodholt, J. & Stein, S. Geophys. Res. Lett. 15, 1081-1084 (1988).
11. Vassiliou, M. S., Hager, B. H. & Raefsky, A. J. Geodynam. 1, 11-28 (1984).
12. Wortel, R. Nature 296, 553-556 (1982).
13. Wortel, R. Geophys. Res. Lett. 13, 34-37 (1986).
14. Wortel, R. & Vlaar, N. J. Pure appl. Geophys. 128, 625-659 (1988).
15. Meade, C. & Jeanloz, R. Science 252, 68-72 (1991).
16. Bina, C. R. & Wood, B. J. J. geophys. Res. 92, 4853-4866 (1987).
17. Molnar, P., Freedman, C. & Shih, J. F. Geophys. J. R. astr. Soc. 56, 41-54 (1979).
18. Larson, R. L. et al. The Bedrock Geology of the World (map) (Freeman, New York, 1985).
19. Leg 129 shipboard scientific party Nature 345, 112 (1990).
20. Jarrard, R. D. Rev. Geophys. 24, 217-284 (1986).
21. Toksöz, M. N., Sleep, N. H. & Smith, A. T. Geophys. J. R. astr. Soc. 35, 285-310 (1973).
22. DeMets, C., Gordon, R. G., Argus, D. F. & Stein, S. Geophys. J. Int. 101, 425-478 (1990).
23. Geller, R. J. Bull. seism. Soc. Am. 66, 1501-1523 (1976).
24. Press, W. H., Flannery, B. P., Teukolsky, S. A. & Vetterling, W. T. Numerical Recipes (Cambridge University Press, 1987).

Spatial structure and chaos in insect population dynamics

Michael P. Hassell*, Hugh N. Comins*
& Robert M. May†

* Department of Biology and Centre for Population Biology, Imperial College, Silwood Park, Ascot, Berkshire SL5 7PY, UK
† Department of Zoology, University of Oxford, Oxford OX1 3PS, UK

MOST environments are spatially subdivided, or patchy, and there has been much interest in the relationship between the dynamics of populations at the local and regional (metapopulation) scales[1]. Here we study mathematical models for host–parasitoid interactions, where in each generation specified fractions (μ_N and μ_P, respectively) of the host and parasitoid subpopulations in each patch move to adjacent patches; in most previous work, the movement is not localized but is to any other patch[2]. These simple and biologically sensible models with limited diffusive dispersal exhibit a remarkable range of dynamic behaviour: the density of the host and parasitoid subpopulations in a two-dimensional array of patches may exhibit complex patterns of spiral waves or spatially chaotic variation, they may show static 'crystal lattice' patterns, or they may become extinct. This range of behaviour is obtained

with the local dynamics being deterministically unstable, with a constant host reproductive rate and no density dependence in the movement patterns. The dynamics depend on the host reproductive rate, and on the values of the parameters μ_N and μ_P. The results are relatively insensitive to the details of the interactions; we get essentially the same results from the mathematically-explicit Nicholson–Bailey model of host-parasitoid interactions, and from a very general 'cellular automaton' model in which only qualitative rules are specified. We conclude that local movement in a patchy environment can help otherwise unstable host and parasitoid populations to persist together, but that the deterministically generated spatial patterns in population density can be exceedingly complex (and sometimes indistinguishable from random environmental fluctuations).

Insect parasitoids lay their eggs on, in or near the bodies of other arthropods, and the parasitoid larvae kill the host as they feed on it. The dynamics of systems with discrete but synchronized generations of hosts and parasitoids are thus simpler than most other prey-predator associations (see equation (1)) and make convenient systems for study[3]. Theoretical and empirical studies of predator-prey systems in general have contributed much to the emerging consensus that spatial patchiness is important to the understanding of regulation and persistence of many natural populations[4-11]. Recent work on the dynamics of host-parasitoid interactions in particular has also begun to provide a unifying framework for understanding the magnitude of the patch-to-patch variability in levels of parasitism that is required for the population as a whole to persist[12-14]. Little attention, however, has been given to the importance of the type of dispersal between units of local population density (but see refs 10, 11). This work is devoted largely to this question, and to the surprising answers that can emerge when dispersing individuals only move locally (rather than spreading globally, as in most previous work).

In a homogeneous environment, host-parasitoid dynamics may be described by a pair of first-order difference equations

$$N_{t+1} = \lambda N_t f(N_t, P_t) \qquad (1a)$$

$$P_{t+1} = q N_t (1 - f(N_t, P_t)). \qquad (1b)$$

Here N_t and P_t are, respectively, the host and parasitoid population sizes in generation t; λ is the average number of
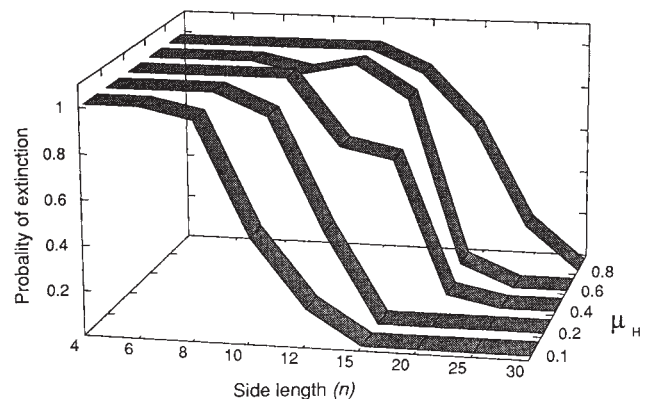

FIG. 1 Extinction probabilities for the specific model described in the text, in relation to the numbers of patches in a square grid of side length (n) and the fractions of hosts dispersing to neighbouring patches (μ_N) (μ_P = 0.89, $\lambda = 2$, reflective boundaries). Extinction is measured as the proportion of 20 replicates failing to persist over 2,000 generations. Each replicate is started by setting nonzero population densities in only the third patch from the left in the top row. The same 20 pairs of initial host and parasitoid densities are used for all the parameter combinations. Local extinction occurs by numeric underflow (densities less than about 10^{-45}); however, the results are robust when local extinction thresholds for both hosts and parasitoids are modelled explicitly.

offspring produced by an unparasitized host (assumed to be independent of host density; stability considerations will be more complicated when λ has significant density-dependence); $f(N, P)$ is the fraction of hosts that escape parasitism; and q is the average number of female parasitoids emerging from each host parasitized. If parasitoids search randomly and independently, then we get the classic Nicholson–Bailey model ($f = \exp(-aP)$), which is unstable with diverging oscillations[15]. If we suppose that the environment consists of a square grid containing many patches, then the dynamics involves two steps. In the first step, we apply equation (1) to the subpopulations in each patch, to find how many hosts and parasitoids will emerge in the next generation (the 'escape function' f in any one patch may be of simple Nicholson–Bailey form, corresponding to random search within patches, or it may be more complex). In the second step, we allow for dispersal, distributing some fixed fraction (μ_N) of the hosts and (μ_P) of the parasitoids in each patch among other patches, according to some specified rules. In most previous studies, the dispersing individuals are distributed according to some particular statistical distribution (often a negative binomial) over all other patches. In these cases, overall population densities will tend to be stable provided the coefficient of variation squared of the density of searching parasitoids in the vicinity of each host exceeds approximately unity (the '$CV^2 > 1$ rule')[12-14]. This approximate criterion only depends on the degree of heterogeneity in the risk of parasitism between individual hosts[16]; thus spatial patterns of parasitism that are directly or inversely related to host abundance per patch, or that show no such covariance, can all contribute to population persistence in the same way[14]. When we look at the two-dimensional spatial array of densities of host and parasitoid subpopulations generated by such 'global movement' models, we simply see the spatially stochastic pattern corresponding to the underlying statistical distribution used to describe the dispersal process.

Suppose, however, rather than the dispersing individuals from each patch entering a 'pool' for global dispersal, they diffuse outwards, in this case by equal distribution among the eight nearest neighbours of that patch in the square array. To lay bare this effect alone, moreover, let us suppose parasitism is random in each patch ($f = \exp(-aP)$ in equation (1)). For specified values of the parameters λ, μ_N and μ_P (the parameters q and a are principally scaling factors and otherwise do not affect the dynamics), we now have a purely deterministic model for the spatial and temporal dynamics of this host–parasitoid association. We have conducted extensive numerical and analytical studies of this system in which the size of the $n \times n$ array of patches is varied. The results are as follows.

If the number of patches is too small, then the underlying instability of the simple Nicholson–Bailey model in each patch

FIG. 2 Photographs illustrating the different patterns of spatial dynamics obtained from the specific model (a–c) and the cellular automaton model (d) discussed in the text. Each photograph is a snapshot in time with the colour coding representing different relative abundances of hosts and parasitoids within a patch. a, Typical 'spiral waves' obtained in the spiral region of Fig. 3. b, The 'crystal lattice' pattern obtained for $\mu_P \to 1$ and small μ_N (top left of Fig. 3). This pattern settles to a completely static mosaic of high density and low density patches; there is variation within the high and low density categories, although this variation does not show up with our colour-coding. c, Spatially erratic ('chaotic') patterns obtained in the chaos region of Fig. 3. d, A typical spatial pattern generated from the cellular automaton in which the movement rules correspond qualitatively to the specific model. The automaton has nine states, labelled A to I; movement to the next state in cyclic order is automatic, except that state A (empty) moves to state B only in the presence of at least one neighbouring B (modelling host colonization), and state D moves to state E only in the presence of an F neighbour (modelling parasitoid colonization). Only the four orthogonal nearest neighbour cells are used. Variant automata (exhibiting spirals, crystals and other behaviour) are generated by using eight nearest neighbours, and by changing the required neighbours for $A \to B$ to C or D and for $D \to E$ to D, F, G or H. These changes affect the velocities of the colonization wavefronts of hosts and parasitoids, and are analogous to changes in μ_N and μ_P in the specific model.
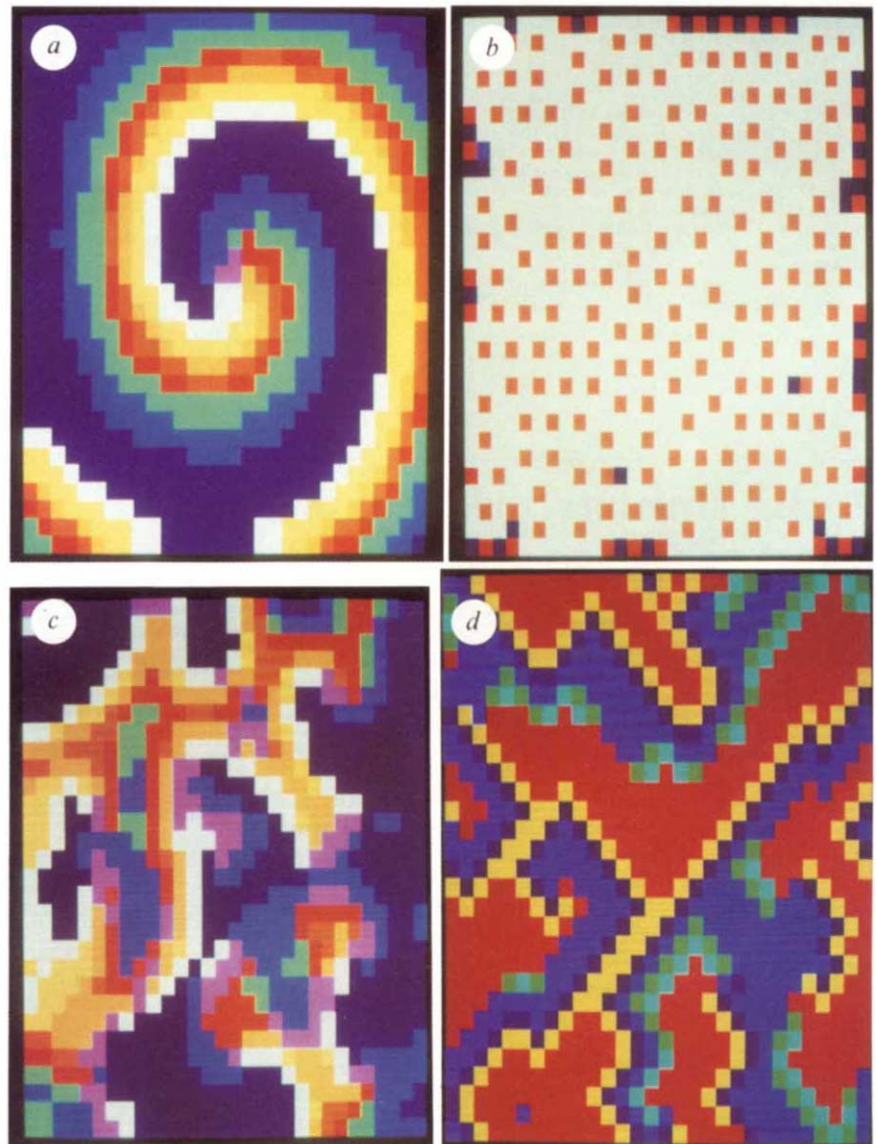
eventually drives the entire system to extinction; there are diverging oscillations in local densities, and first host and then parasitoid populations are extinguished. What is meant by 'too small' an array depends on the fraction of hosts and parasitoids that leave their home patch each generation (μ_N and μ_P, respectively), and on the host's intrinsic growth rate, λ. Figure 1 illustrates this, showing the proportion of simulations that result in extinction as a function of μ_N and of the side-length, n, of the array of patches. For instance, with $\mu_N = 0.1$ all the arrays of 6×6 or smaller result in extinction, all of 15×15 or greater persist, whereas for intermediate-sized arrays there is an element of chance (with some initial configurations leading to persistence and others to extinction, sometimes after quite long times). Higher degrees of host movement (higher μ_N) make persistence less easy and, as ever, persistence is also more difficult for very large λ. These results are all fairly insensitive to whether one assumes periodic, reflexive, or absorbing boundary conditions on the array (the details of boundary conditions will be described elsewhere (H.N.C, M.P.H. and R.M.M., manuscript in preparation)).

The persisting deterministic systems settle to one of three broadly-distinguishable patterns.

The first shows patterns of spiral waves. Figure 2a shows a snapshot in time of such a pattern (assuming reflection at the boundaries). Over time, the waves spiral outwards, collide, and perform all manner of manoeuvres, but all the time retaining their overall wavelength and the spiral pattern. Previous studies of the spatial dynamics of prey–predator interactions in continuous time (as distinct from our discrete-time interactions with difference equations) have employed nonlinear 'reaction-diffusion' differential equations, and have found stable wave patterns (see, for example, ref. 9 for a study of goldenrod aphids and ladybug beetles, and ref. 17 for a more general review). The complex spiral waves in Fig. 2a are, however, new in this context.

The second pattern, attained for a relatively restricted range of values of μ_P near 1 and small μ_N, gives a completely static 'crystal lattice', as illustrated in Fig. 2b. Analytical results support
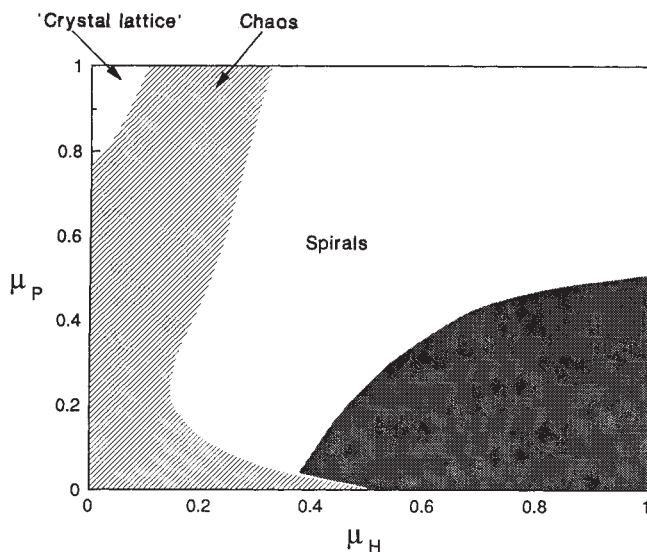

FIG. 3 Diagram showing the dependence of the type of persistent spatial pattern observed on μ_N and μ_P, for $n = 30$ and $\lambda = 2$. The boundaries are obtained by simulation, and are approximate (and partly subjective). The shaded area represents parameter combinations for which the persistent spatial pattern is unlikely to be established by starting the simulation with a single non-empty patch (as described in Fig. 1 caption). Spirals may be established in these cases by starting with a lower μ_N and increasing it after 100 to 200 generations. Non-persistence occurs for some combinations with very small μ_N or μ_P; this area is imperceptible in the figure.

the finding that these 'crystal lattice' patterns need not be neatly periodic in space; they can be deformed, spatially irregular lattices, while retaining their essential property of being temporally static (the static 'crystal lattices' are, moreover, only possible if λ is small enough—specifically, $\lambda < e = 2.7$).

The third pattern, illustrated by Fig. 2c, is one of spatial chaos, with the spatially erratic pattern changing from generation to generation in an apparently unpredictable way. The underlying equations, however, are rigidly deterministic, with no random or unpredictable elements whatsoever (in contrast to the spatial patterns of the 'global dispersal' models[18,19], in which the distribution of the dispersing individuals among patches is stochastic, described by some statistical distribution). Figure 2c is an example of spatial chaos, generated by a simple and biologically motivated model that is wholly deterministic; the temporal sequence of successive patterns is even more striking.

Figure 3 indicates roughly which of the three characteristic patterns we may expect to see for particular values of μ_N and μ_P, assuming a 30×30 array of patches. This figure is necessarily impressionistic because the 'crystal lattice' pattern of Fig. 2a gradually shades into the spatial chaos of Fig. 2c, which in turn gradually shades into the spiral wave pattern of Fig. 2b as μ_N increases and μ_P decreases. Finally, no matter how large the two-dimensional array of patches, the system goes extinct if $\mu_N \to 0$ or $\mu_P \to 0$.

Turning back to the overall population dynamics, these results for models with local movement may be related to the previously discussed results based on global dispersal. Obviously, the results support the general point that patchiness, coupled with local movement among patches, can stabilize host–parasitoid associations (note that the underlying interaction in any one patch is by itself highly oscillatorily unstable). A. M. De Roos, E. McCauley and W. G. Wilson have independently made this point in an analysis of the overall dynamics of host–parasitoid systems similar to those studied here (personal communication). In more detail, we find that the rough stability rule mentioned above, $CV^2 > 1$, is supported in a qualified way by the models in our study: the associations which persist by virtue of spatial chaos or spirals (and which have roughly steady overall population values) consistently have CV^2 slightly greater than one. On the other hand, static crystal lattices have $CV^2 \ll 1$.

How robust are these results? To what extent do the patterns in Fig. 2, and their parameter-dependence in Fig. 3, depend on the detailed assumption of Nicholson–Bailey dynamics (with random search) within each patch? We could attempt to answer these questions by exploring other specific forms of the function $f(N, P)$ in equation (1). This is the procedure that has usually been adopted in past studies of this general kind[3]. Instead, we adopt the more novel approach of using a cellular automaton to explore the robustness of our conclusions about the population dynamics[20-22]. In the work described above, we used an explicit equation for the dynamics in each patch and explicit formulae describing movement to neighbouring patches. To display the results, the two-dimensional arrays of population densities were colour-coded in Fig. 2 by assigning nine colours to characterize nine categories of patches defined by dividing each population density into three classes ('very low, medium, high'). For a cellular automaton approach, we abandon detailed host and parasitoid population values, and acknowledge only these nine qualitative categories of patch densities. We then define a set of 'movement rules' that specify the colour of each patch next generation in relation to its present colour and the colour of its eight neighbours. These rules are qualitative embodiments of the workings of dynamics within a patch and subsequent dispersal patterns.

Thus defined, our cellular automata give results qualitatively very similar to those of the detailed models. Arrays that are too small lead to extinction. Large enough arrays can give crystal lattices, or spiral waves, or spatial chaos (in which deterministic rules, with no random elements, give apparently random spatial

257

patterns). Figure 2*d* is a representative example, being the cellular automaton analogue of Fig. 2*a* with spiral waves moving as 'fronts' across the patchy environment.

In a homogeneous environment, host–parasitoid associations with discrete generations will not persist unless the parasitoids search nonrandomly, or unless host or parasitoid populations exhibit some form of inherent density-dependent effects. In a subdivided environment, such associations can persist without any explicit density-dependences, and with parasitoids searching randomly within patches, provided the hosts in each generation are sufficiently aggregated in their distribution among patches and there is sufficient variability in the density of searching parasitoids in the vicinity of individual hosts. We have extended these results to show that purely deterministic processes, whereby some constant fractions of hosts and parasitoids (μ_N and μ_P, respectively) move to immediately neighbouring patches in each generation, can also lead to overall persistence, even when parasitoids search randomly within patches and no explicit density-dependent mechanisms are present. The densities of host and parasitoid subpopulations in a two-dimensional ($n \times n$) array of patches can exhibit spiral waves, or spatial chaos (with deterministic rules generating patterns that are apparently random in time and space), or static-looking 'crystal lattice' patterns, depending on the magnitude of the parameters, μ_N and μ_p, and provided n is big enough. Note that these complex patterns of spatial variation in population density arise even though the environment in our different patches is the same; the patterning is thus intrinsically generated by the interplay of local dispersal and local dynamics. These results seem robust, being true both for conventional mathematical models based on Nicholson–Bailey or similar equations, and for cellular automata based on qualitative rules. We emphasize that these complex patterns in the densities of host and parasitoid subpopulations in individual patches (as shown in Fig. 2*c*) are produced by strictly deterministic rules or equations. In practice, such spatially chaotic patterns may be hard to distinguish from those produced by randomly varying environmental factors. □

1. Gilpin, M. E. & Hanski, I. *Metapopulation Dynamics: Empirical and Theoretical Investigations* (Academic, London, 1991).
2. Taylor, A. D. *Ann. Zool. Fenn.* **25**, 63–74 (1988).
3. Hassell, M. P. *The Dynamics of Arthropod Predator–Prey Systems* (Princeton University Press, Princeton, 1978).
4. Hassell, M. P. & May, R. M. *J. Anim. Ecol.* **42**, 693–726 (1973).
5. Hassell, M. P. & May, R. M. *J. Anim. Ecol.* **43**, 567–594 (1974).
6. Maynard Smith, J. *Models in Ecology* (Cambridge University Press, Cambridge, 1974).
7. Kareiva, P. *Lect. Not. Biomath.* **54**, 368–389 (1984).
8. Kareiva, P. *Nature* **321**, 388–391 (1989).
9. Kareiva, P. & Odell, G. M. *Am. Nat.* **130**, 233–270 (1987).
10. Nachman, G. *J. Anim. Ecol.* **56**, 247–265 (1987).
11. Nachman, G. *J. Anim. Ecol.* **56**, 267–281 (1987).
12. Pacala, S., Hassell, M. P. & May, R. M. *Nature* **344**, 150–153 (1990).
13. Hassell, M. P. & Pacala, S. *Phil. Trans. R. Soc.* **330**, 203–220 (1990).
14. Hassell, M. P., Pacala, S., May, R. M. & Chesson, P. L. *Am. Nat.* **138** (in the press).
15. Nicholson, A. J. & Bailey, V. A. *Proc. Zool. Soc. London* **3**, 551–598 (1935).
16. Chesson, P. L. & Murdoch, W. W. *Am. Nat.* **127**, 696–715 (1986).
17. Murray, J. D. *Mathematical Biology* (Springer, London, 1989).
18. Hassell, M. P. & May, R. M. *Ann. Zool. Fenn.* **25**, 55–61 (1988).
19. Reeve, J. D. *Am. Nat.* **132**, 810–836 (1988).
20. Conway, J. H. *On Numbers and Games* (Academic, London, 1976).
21. Wolfram, S. *Nature* **311**, 419–424 (1984).
22. Crawley, M. J. & May, R. M. *J. theor. Biol.* **125**, 475–489 (1987).

A selective deficit for writing vowels in acquired dysgraphia

Roberto Cubelli

Rehabilitation Department, Ospedale Maggiore, Bologna I-40133, Italy

BRAIN-DAMAGED patients with acquired writing disorders provide important information about the normal processes of spelling and writing[1,2]. Current models indicate that to produce a letter string, its 'abstract' representation is computed and stored in a temporary orthographic buffer, from which it is converted to a verbal code (if the word is to be spelled aloud) or to a physical letter code (if the word is to be written). The stored graphemic representations specify the identity and order of the component letters[3] and their consonant/vowel status[4]. Here I describe the spelling performance of two patients with a selective deficit in writing vowels. When writing words, the first patient omitted all vowels, leaving a blank space between consonants or consonant clusters, whereas the second produced errors that almost exclusively involved vowels. This pattern of performance supports the hypothesis that the consonant/vowel status of graphemes is differentially specified in the spelling process and may be selectively affected after brain damage.

C.F. is a 43-year-old right-handed engineer with eight years of schooling. On 21 September 1990 he suffered an ischaemic infarction which involved the parietal lobe of the left cerebral hemisphere. On the first neuropsychological examination, two weeks after the stroke, he was totally speechless but could communicate by gestures. Auditory verbal comprehension was clinically normal. He wrote with the left hand because of a severe right hemiplaegia. When asked to write his name and the names of his town and of five objects, he omitted all vowels (Fig. 1), leaving a blank space between correctly written consonants. Consonant clusters were preserved and no space was left between letters. C.F. was aware of errors, but did not seem to be able to choose the correct letters. The deficit was transient. In the following days, the patient began to improve and a week later he showed a mild Broca's aphasia with articulatory difficulties and some anomic pauses. Writing performance was almost normal with only sporadic letter substitutions. Patients who leave blank spaces for unavailable letters are not uncommon[5,6], but a specific vowel impairment is completely novel.

C.W. is a 62-year-old right-handed man. He is a retired typographer with eight years of schooling. On 31 August 1990, he suffered an ischaemic infarction in the left frontal subcortical region. He had neither motor nor sensory deficits. C.W. showed a form of transcortical motor aphasia with some difficulties in initiating speech but relatively good auditory–verbal comprehension. Spontaneous speech was severely reduced with perseveration and occasional phonemic and verbal paraphasias, but no articulatory disorders. C.W. showed a specific deficit in writing (Table 1).

His spelling abilities were widely investigated (Table 2). He showed the same level of performance and the same kind of errors independently of input (oral dictation, delayed copying) or output (written spelling, oral spelling, typing) modalities. Writing was not affected by lexical factors (grammatical class, word frequency or abstract quality) or lexicality (words versus non-words). Only stimulus length influenced his performance, with short stimuli being spelled better than longer ones. The number of letters and not the number of syllables seemed to be the critical factor. C.W. made significantly fewer errors in writing capital letters than cursive. This is probably because with capital letters the patient was slower and made more corrections. In any case, the pattern of errors was not different in the two conditions. Direct copying and writing to dictation of single letters and syllables were flawless. C.W. wrote with his (dominant) right hand.

In the entire corpus of responses, 409 letters were produced incorrectly. The most frequent error type was letter substitution ($n = 340$ (83%); for example, dietro (behind) → diatro). Other errors were transpositions ($n = 30$ (7%); for example, caro (dear) → cora), deletions ($n = 26$ (6%); for example, premio